HHS Public Access

Author manuscript

FASEB J. Author manuscript; available in PMC 2022 December 29.

Published in final edited form as:

FASEB J. 2020 November ; 34(11): 14863–14877. doi:10.1096/fj.202001061R.

A critical role for hepatic protein arginine methyltransferase 1 isoform 2 in glycemic control

Yingxu Ma[1,3], **Shanshan Liu**[1], **Heejin Jun**[1], **Jine Wang**[1], **Xiaoli Fan**[5], **Guobing Li**[1], **Lei Yin**[2], **Liangyou Rui**[2], **Steven A. Weinman**[4], **Jianke Gong**[1,5], **Jun Wu**[1,2]

[1]Life Sciences Institute, University of Michigan, Ann Arbor, Michigan 48109, USA.

[2]Department of Molecular & Integrative Physiology, University of Michigan Medical School, Ann Arbor, Michigan 48109, USA.

[3]Department of cardiology, The Second Xiangya Hospital, Central South University, Changsha, Hunan 410013, China.

[4]Department of Internal Medicine and the Liver Center, University of Kansas Medical Center, Kansas City, Kansas 66160, USA.

[5]International Research Center for Sensory Biology and Technology of MOST, Key Laboratory of Molecular Biophysics of MOE, and College of Life Science and Technology, and Huazhong University of Science and Technology, Wuhan, Hubei, 430074, China.

Abstract

Appropriate control of hepatic gluconeogenesis is essential for the organismal survival upon prolonged fasting and maintaining systemic homeostasis under metabolic stress. Here we show protein arginine methyltransferase 1 (PRMT1), a key enzyme that catalyzes the protein arginine methylation process, particularly the isoform encoded by *Prmt1* variant 2 (*PRMT1V2*), is critical in regulating gluconeogenesis in the liver. Liver-specific deletion of *Prmt1* reduced gluconeogenic capacity in cultured hepatocytes and in the liver. *Prmt1v2* was expressed at a higher level compared to *Prmt1v1* in hepatic tissue and cells. Gain-of-function of PRMT1V2 clearly activated the gluconeogenic program in hepatocytes via interactions with PGC1α, a key transcriptional coactivator regulating gluconeogenesis, enhancing its activity via arginine methylation, while no effects of PRMT1V1 were observed. Similar stimulatory effects of PRMT1V2 in controlling gluconeogenesis were observed in human HepG2 cells. PRMT1, specifically PRMT1V2, was stabilized in fasted liver and hepatocytes treated with glucagon, in a PGC1α-dependent manner. PRMT1, particularly *Prmt1v2*, was significantly induced in the liver of streptozocin-induced type 1 diabetes and high fat diet-induced type 2 diabetes mouse models and liver-specific *Prmt1* deficiency drastically ameliorated diabetic hyperglycemia. These findings reveal that

Correspondence: College of Life Science and Technology, Key Laboratory of Molecular Biophysics of MOE, Huazhong University of Science and Technology, Wuhan, Hubei, 430074, China. jiankeg@umich.edu (J. Gong). Life Sciences Institute, University of Michigan, Ann Arbor, MI, 48109, USA. wujunz@umich.edu (J. Wu).

Author contributions

YM and JWu conceived the project and designed the study. YM, SL, HJ, JWang, XF, GL, JG performed the experiments and analyzed the data. LY, LR and SAW provided reagents and discussions. YM and JWu wrote the manuscript. JWu oversaw the study.

Declaration of competing interest

The authors declare no competing interests.

PRMT1 modulates gluconeogenesis and mediates glucose homeostasis under physiological and pathological conditions, suggesting that deeper understanding how PRMT1 contributes to the coordinated efforts in glycemic control may ultimately present novel therapeutic strategies that counteracts hyperglycemia in disease settings.

Keywords

PRMT1 variant 2; Glycemic control; Liver function; Diabetic hyperglycemia

Introduction

Glucose homeostasis is of great importance for survival and metabolic health in general. Blood glucose levels must be maintained within a narrow range to avoid hypoglycemia during periods of fasting and hyperglycemia after calorie overload. Liver plays a key role in the regulation of systemic glucose levels because hepatic glucose production contributes to 80% of total endogenous glucose production (1). Hepatic glycogenolysis is mainly responsible for glucose production in the short-term fasting but gluconeogenesis is of much greater importance during prolonged fasting (2). Hepatic gluconeogenesis is mainly controlled by the availability of substrates and the rate-limiting enzymes phosphoenolpyruvate carboxykinase 1 (encoded by *Pck1*) and glucose-6-phosphatase (encoded by *G6pc*). This process is tightly modulated through the actions of insulin and glucagon, which coordinately respond to nutrient status. In patients with diabetes and other metabolic disorders, inappropriate activation of gluconeogenesis and development of insulin resistance renders hyperglycemia.

Peroxisome proliferative activated receptor-γ co-activator 1 (PGC1α) was originally identified in brown fat, regulating adaptive thermogenesis as a transcriptional coactivator (3). Further investigation revealed that PGC1α can be induced by cyclic adenosine monophosphate (cAMP) in primary hepatocytes and was significantly induced in the liver by fasting (4). PGC1α is the master modulator of hepatic metabolism through regulation of gluconeogenesis, lipid catabolism, mitochondrial biogenesis via interactions with many key factors, including forkhead transcription factor (FOXO1), hepatocyte nuclear factor 4α (HNF4α) and Sirtuin 1 (SIRT1) (4-7). The activity of PGC1α is closely monitored and tightly controlled at transcriptional and posttranslational levels to accommodate its versatile functions in various physiological processes (8), including arginine methylation (9).

Methylation of arginine residues is a common post-translational modification and is regulated by a family of gene products called protein arginine methyltransferases (PRMTs) (10). PRMTs are classified as type °C (PRMT1, 2, 3, 4, 6, and 8), type °C (PRMT5 and 9) and type °C (PRMT7) on the basis of their methylation manner (11). PRMT1 is the predominant member of the PRMT family, contributing to around 85% of protein arginine methylation in mammalian cells and tissues. It has been reported that PRMT1 modulates insulin signaling (12), maintains cardiac function (13), mediates lipogenesis in the liver (14), and regulates thermogenesis in fat (15). *Prmt1* has different splicing variants with distinct subcellular localization, substrate specificity, and enzyme activity (16). Among all these

isoforms, *PRMT1V1* and *PRMT1V2* are the two main variants in normal human tissues (16). The difference between these two isoforms is that *PRMT1V1* has a chromosome region maintenance 1/exportin1/Exp1/Xpo1 (CRM1)-dependent nuclear export sequence which is coded by exon 2 (15, 16).

In this study, multiple lines of in vitro and in vivo evidence generated from gain- and loss-of-function models strongly support the hypothesis that PRMT1, variant 2 in particular, plays an essential role in regulating hepatic gluconeogenesis via interactions with PGC1α. PRMT1V2 was induced in the liver of mouse models mimicking diabetes and other metabolic disorders where pathological hyperglycemia was observed. Mice with hepatocyte-specific *Prmt1* deletion displayed less elevated blood glucose levels and improved glucose homeostasis when challenged with streptozocin or high fat diet (HFD), indicating inhibition of hepatic PRMT1 activity may represent therapeutic opportunities counteracting inappropriate gluconeogenesis in human diseases.

Materials and Methods

Reagents

Glucagon (G2044), forskolin (F6886), insulin (I5500, for in vitro studies), dexamethasone (D4902), fetal bovine serum (FBS) (F0926), cycloheximide (CHX; C4859), MG132 (M7449), ammonium chloride (NH_4Cl; A9434), and streptozocin (STZ; S0130) were purchased from Sigma-Aldrich. Insulin (NDC 0002-8215-01, for in vivo studies) was purchased from Eli Lilly. Hanks' Balanced Salt Solutions (HBSS; SH3058802) was purchased from Thermo Fisher Scientific. Dulbecco's Modified Eagle Medium/Nutrient Mixture F-12 GlutaMAX (DMEM/F12 GlutaMAX) (10565-042), DMEM (11995073), DMEM-low glucose (11885084), and penicillin streptomycin solution(15140122) were purchased from Life Technologies. Collagenase Type IV (LS004188) was purchased from Worthington Biochemical. Polyethylenimine (PEI; linear, molecular mass of 25 kDa; 23966-1) was purchased from Polysciences, Inc.

Animal studies

All the mouse studies were conducted according to the protocol reviewed and approved by the Institutional Animal Care and Use Committee at the University of Michigan. All mice were housed under 12-hour light/12-hour dark cycle with an *ad libitum* chow diet (5L0D; PicoLab Laboratory Rodent Diet) unless otherwise indicated. The C57BL/6J (000664) and *Albumin*-Cre (003574) mice were obtained from the Jackson Laboratory. *Prmt1*$^{fl/fl}$ mice were obtained from Dr. Steven A. Weinman. The conditioned alleles lead to Cre-mediated deletion of exon 4 and 5 of *Prmt1* gene (17). Liver-specific *Prmt1* KO mice (*Alb-Cre*;*Prmt1*$^{fl/fl}$) were generated by crossing *Prmt1*$^{fl/fl}$ and *Alb-Cre* mice. For the fasting experiments, mice were fasted during the dark period for indicated time. Blood glucose levels were measured in tail blood by using the OneTouch Ultra Glucometer (Lifescan). For adenovirus infusion studies, indicated adenoviruses were injected into anesthetized mice through tail vein. For STZ studies, mice were intraperitoneally injected with either vehicle or 100 mg per kg body weight per day STZ for one week. For HFD-induced obesity study, mice were singly housed on either a chow diet or a HFD that consists of 45% of calories

from fat (D12451, Research Diets) for indicated time. Over this period, body weights and food intake were measured weekly. For diet-induced nonalcoholic steatohepatitis (NASH) study, mice were singly housed on either a chow diet or Gubra Amylin NASH (GAN) diet (D09100310, Research Diets). Over this period, body weights and food intake were measured weekly. Both male and female were used in this study and similar results were observed in both genders.

Quantitative real-time PCR

Total RNA was extracted from cells and tissues using TRI reagent (T9424, Sigma-Aldrich) according to the manufacturer's instructions. cDNA was synthesized using M-MLV Reverse Transcriptase (28025021, Life Technologies). Quantitative real-time PCR (qPCR) reactions were performed with SYBR Green (4368708, Thermo Fisher Scientific) on a QuantStudio 5 Real Time PCR system (Thermo Fisher Scientific). Results were analyzed by using the $2^{-\Delta\Delta Ct}$ method and normalized to levels of TATA-box binding protein (*Tbp*). All qPCR primer sequences are listed in Supplementary Table.

Western blot

Total protein from cells and liver tissue was extracted in ice-cold radioimmunoprecipitation assay buffer (RIPA buffer) (150 mM NaCl, 50 mM Tris-HCl pH 8.0, 5 mM EDTA, 0.5% sodium deoxycholate, 0.1% SDS, 1% NP-40) supplemented with protease inhibitor cocktail (Sigma-Aldrich). Protein concentration was measured by DC protein assay reagents (Bio-Rad Laboratories) in SpectraMax M3 multi-mode microplate reader (Molecular Devices). Protein lysate was subjected to SDS-PAGE and transferred to polyvinylidene fluoride (PVDF) membranes. After incubation with blocking buffer (5% nonfat milk in 1% TBS with Tween 20) for 1 hour, the membranes were probed with primary anti-PRMT1 (Cell Signaling Technology, catalog 2449S), anti-HSP90 (Cell Signaling Technology, catalog 4874S), anti-HA (Cell Signaling Technology, catalog 3724), anti-α-tubulin (Cell Signaling Technology, catalog 2144), anti-Adme-R (Cell Signaling Technology, catalog 13522), anti-pAkt (Cell Signaling Technology, catalog 9271S), anti-Akt (Cell Signaling Technology, catalog 9272), and anti-Histone H3 (Active motif, catalog 39763). Secondary antibody linked with horseradish peroxidase was diluted in 5% nonfat milk in 1% TBS with Tween 20 and incubated for 2 hours at room temperature. The blots were developed by ECL (Bio-Rad Laboratories, 1705061). Quantification of immunoblot analyses was performed using Quantity One (Bio-Rad).

Subcellular fractionation

Liver tissue was minced in ice-cold cytoplasm extraction buffer (20 mM HEPES, 1 mM EDTA, 10 mM NaCl, 2 mM $MgCl_2$, 0.25% NP-40) supplemented with protease inhibitor cocktail (Sigma-Aldrich) whereas cells were scraped in ice-cold cytoplasm extraction buffer. The homogenate was vortexed for 15 seconds followed by 5 minute incubation at 4°C for 6 times. The lysate was centrifuged at 5000*g* at 4°C for 5 minutes to get the supernatant containing cytoplasmic fraction. The pellet after centrifugation was vortexed for 15 seconds and incubated at 4°C for 10 minutes in ice-cold nuclear extraction buffer (20 mM HEPES, 1 mM EDTA, 420 mM NaCl, 2 mM $MgCl_2$, 0.25% NP-40, 25% glycerol) supplemented with

protease inhibitor cocktail (Sigma-Aldrich). The homogenate was centrifuged at 14,000*g* at 4°C for 5 minutes to get the supernatant containing nuclear fraction.

Immunoprecipitation

Hepa 1-6 cells were infected with indicated adenoviruses or transiently transfected with indicated plasmids. At 48 hours following infection or transfection, cells were lysed with ice-cold RIPA buffer on a shaker at 4°C for 1 hour. The lysate was centrifuged at 14,000*g* for 15 minutes at 4°C to pellet debris and the supernatant was transferred into a fresh Eppendorf tube. After quantification by DC assay, 1 mg of protein for each group was incubated with anti-PGC1α (Millipore, catalog ST1202) overnight at 4°C with rotation. Five percent of the lysate was saved as input. Thirty microliters of protein G-agarose (Santa Cruz Biotechnology, catalog sc-2002) was washed with RIPA buffer 3 times and then added into protein lysate following rotation at 4°C for 3 hours. The beads were pelleted by quick spin and washed with RIPA buffer 3 times. After removing supernatant, 30 μL of sample buffer was added to elute the immunoprecipitated proteins followed by boiling at 98°C for 5 minutes. The immunoprecipitated protein was subjected to immunoblotting as described above.

Tolerance tests

For pyruvate tolerance test (PTT), mice were fasted for 16 hours and then intraperitoneally injected with sodium pyruvate (1.75 g/kg). For glucose tolerance test (GTT), mice were fasted for 16 hours and then intraperitoneally injected with glucose (1 g/kg). The blood glucose levels were measured in tail blood at indicated time points by using the OneTouch Ultra Glucometer (Lifescan).

Cell culture

Mouse primary hepatocytes were isolated and cultured as previously reported (15). In brief, the liver was perfused with washing buffer (HBSS buffer supplemented with 0.5 mM EGTA pH 7.4 and 25 mM HEPES pH 7.4) and then with digestion medium (DMEM-low glucose supplemented with 1% penicillin-streptomycin, 15 mM HEPES pH 7.4, and 100 U/mL collagenase IV) via the inferior vena cava after the anesthesia of the mouse. After dispersing the cells, they were filtered by using a prechilled BD disposable falcon tube nylon filter. Hepatocytes were washed twice by using isolation medium (DMEM/F12 GlutaMAX supplemented with 10% FBS, 1% penicillin-streptomycin, 1 μM dexamethasone and 0.1 μM insulin) and seeded on collagen coated 12-well plates at 3×10^5 cells/mL with the isolation medium. One hour after plating, the medium was changed to culture medium (DMEM-low glucose supplemented with 10% FBS, 1% penicillin-streptomycin, 0.1 μM dexamethasone, and 1 nM insulin). Cells will be serum starved for 24 hours before treatments (such as glucagon).

Hepa 1-6 cells and HepG2 cells were obtained from ATCC and maintained in DMEM supplemented with 10% FBS and 1% penicillin-streptomycin. Particularly, HepG2 cells were seeded on culture plates coated with type I rat tail collagen (CB354249, Fisher Scientific).

Histology

Liver tissues were fixed in 10% formalin at 4°C overnight. Paraffin embedding and hematoxylin and eosin (H&E) staining were performed by the University of Michigan Comprehensive Cancer Center Research Histology and Immunoperoxidase Laboratory. Images were obtained by using LEICA DM2000.

Adenovirus production

Adenoviruses that overexpress GFP, CRE, PGC1α (18), HA-PRMT1V1, and HA-PRMT1V2 (15) were generated as previously described. Adenoviruses expressing shRNA against *Ppargc1a* (6) and *PRMT1* (15) were produced as previously described. Media were freshed 16-24 hours after infection and high efficiency of virus transduction that exceeded 90% was verified by the number of GFP-positive cells under fluorescence microscope.

Luciferase reporter assays

Plasmids expressing PRMT1V1, PRMT1V2 (15), PRMT1V2-G98R (19, 20), FOXO1 (21), PGC1α (18), PGC1α-ΔE, PGC1α-R3K (9) and the *Pck1* promoter luciferase reporter (4) were described previously. Hepa 1-6 cells or HepG2 cells were seeded into 12-well plates and transiently transfected with plasmids expressing PGC1α (909 ng), PGC1α-ΔE (909 ng), PGC1α-R3K (909 ng), or FOXO1 (909 ng) and/or PRMT1V1 (909 ng), PRMT1V2 (909 ng) or PRMT1V2-G98R (909 ng) by using PEI method together with *Pck1* promoter luciferase reporter construct (90.0 ng) and *Renilla* luciferase reporter construct (10 ng) unless otherwise specified. Cells were lysed 48 hours after transfection. Luciferase activity was measured by a luciferase assay kit (PR-E1941, Promega) according to the manufacturer's recommendations by using a Perkin Elmer Enspire Model 2300 Multilabel Microplate Reader (PerkinElmer). Firefly luciferase activity was normalized to *Renilla* luciferase activity.

Statistics

Data are presented as mean ± SEM. Two-tailed unpaired Student's *t* test was used for comparison of two genotypes or treatments. One-way ANOVA or 2-way ANOVA was performed to compare 3 or more groups, as indicated in the figure legends. All the statistical analyses were performed using SPSS (IBM).

Results

Hepatic *Prmt1* deficiency renders impaired gluconeogenesis in the liver

To investigate the role of PRMT1 in regulating hepatic glucose metabolism, we first examined wild-type (WT) mice subjected to fasting for 16 hours. As expected, mice in the fasted state had lower body weights and reduced blood glucose levels compared to mice with free access to food (Figure 1A). qPCR analyses revealed that expression levels of key gluconeogenic genes, including *Pck1*, *G6pc*, *Ppargc1a*, and CCAAT/enhancer binding protein beta (*Cebpb*), were elevated in the liver isolated from mice after overnight fasting compared to those of fed controls (Figure 1A). It is of great interest that fasting significantly increased global asymmetric arginine dimethylation with increased PRMT1

expression on the protein level but not transcriptionally in the liver (Figure 1, A and B). To mechanistically investigate the posttranscriptional induction of PRMT1 expression in the liver in the fasting state, a cycloheximide chase experiment was performed to reveal whether this is due to changes in the rate of protein degradation. Treatment with gluconeogenic stimulating hormone, glucagon, dramatically extended the half-life of PRMT1 from 1.6 hours to 3 hours when primary hepatocytes from WT mice were treated with cycloheximide, a commonly used protein synthesis inhibitor (22) (Figure 1C). Further investigation revealed that increased PRMT1 protein accumulation was observed in the primary hepatocytes treated with a proteasome inhibitor MG132 (22) but not NH_4Cl, a lysosome inhibitor (23), suggesting that proteasomal pathways may be involved (Supplementary Figure 1, A and B).

In addition to being stimulated by glucagon after prolonged fasting, gluconeogenesis is also governed by the suppressive effects of insulin postprandially. Reduced suppression of hepatic glucose production rendered by insulin resistance is one of key causes for hyperglycemia observed in type 2 diabetes (24). Therefore, we next investigated whether insulin is also involved in the regulation of hepatic PRMT1. WT mice were subjected to fasting for 16 hours, followed by intraperitoneal injection with insulin. Insulin treatment did not lead to changes in PRMT1 mRNA or protein levels (Supplementary Figure 1, C and D). Similarly, no changes were observed in PRMT1 mRNA and protein in vitro in primary hepatocytes treated with insulin (Supplementary Figure 1, E and F), indicating minimal regulatory effects through insulin in this context.

To determine whether *Prmt1* is required in the hepatic gluconeogenesis, we generated liver-specific *Prmt1* KO mice (*Alb-Cre*;*Prmt1*$^{fl/fl}$) by crossing *Prmt1*$^{fl/fl}$ mice with *Albumin*-Cre mice. Hepatocyte-specific deletion of *Prmt1* did not cause any gross abnormality under the basal conditions. *Alb-Cre*;*Prmt1*$^{fl/fl}$ mice showed no differences in body weight and morphological architecture in the liver compared with *Prmt1*$^{fl/fl}$ controls (Figure 1, D and E). *Prmt1* deletion was confirmed by qPCR in the liver and no deletion was detected in other tissues that express *Prmt1* (Figure 1F). Additionally, no other *Prmts* were induced to compensate for the loss of *Prmt1* expression in the liver (Supplementary Figure 2A). Western blot analyses further confirmed PRMT1 deletion in the liver with significantly reduced global asymmetric arginine dimethylation (Figure 1G), consistent with the notion that PRMT1 plays a predominant role in the liver among all the PRMTs (25). *Alb-Cre*;*Prmt1*$^{fl/fl}$ mice exhibited no changes in gluconeogenic gene expression in the liver under the fed state (Figure 1H). It has previously been reported that deletion of *Prmt1* in the liver may influence cellular response to stresses rendered by environmental insults such as alcohol (26). Decreased expression of oxidative stress response genes (*Sod1* and *Sod2*), increased expression of proliferation markers (*Cyclin B1* and *c-Myc*) and comparable expression of genes regulating inflammation, cell death and fibrosis were observed in the liver of *Alb-Cre*;*Prmt1*$^{fl/fl}$ mice compared to that in the *Prmt1*$^{fl/fl}$ controls under basal conditions (ad lib) (Supplementary Figure 2B), consistent with previous observations (26). After overnight fasting, *Alb-Cre*;*Prmt1*$^{fl/fl}$ mice had lower blood glucose levels and decreased expression of gluconeogenic genes compared to littermate control mice (Figure 1, I and J). Yet, fasting did not result in changes in the expression pattern of the stress response genes between the two genotypes (Supplementary Figure 2C), suggesting the blunted gluconeogenesis in the *Prmt1*-deleted liver after fasting was mediated through a specific

regulatory signaling pathway rather than due to global defects or organ failure. PTT revealed that hepatic gluconeogenesis was impaired after the deletion of *Prmt1* (Figure 1K). It has been reported that global haploinsufficiency of *Prmt1* resulted in impaired gluconeogenesis and significant reduction of PRMT1 protein levels in the liver (27). However, no differences in the expression of gluconeogenic genes were observed in the liver of *Alb-Cre*;*Prmt1*$^{fl/+}$ mice compared to those of *Prmt1*$^{fl/fl}$ mice after overnight fasting. Furthermore, western blot analyses revealed that PRMT1 protein levels were comparable in the liver from *Alb-Cre*;*Prmt1*$^{fl/+}$ mice to those of littermate *Prmt1*$^{fl/fl}$ mice controls (Supplementary Figure 2, D and E).

Similar to what was observed in the *Alb-Cre*;*Prmt1*$^{fl/fl}$ mice where *Prmt1* was deleted developmentally, acute hepatic deletion of *Prmt1* mediated by adenoviral expression of recombinase Cre led to lower fasting blood glucose, less induced hepatic gluconeogenic gene expression after fasting and less glucose production upon pyruvate challenges with no gross differences and morphological changes in the liver under ad lib conditions (Supplementary Figure 3, A-H, and data not shown). The cell-autonomous regulation of hepatic gluconeogenesis through PRMT1 was further confirmed by the observation that *Prmt1* deletion significantly blunted the glucagon-mediated induction of *Pck1*, *G6pc*, *Ppargc1a*, and *Cebpb* in the primary hepatocytes (Supplementary Figure 3, I and J).

We next investigated whether the effects of PRMT1 on gluconeogenesis are conserved in human using a loss-of-function model (Figure 1L). Treatment of glucagon plus forskolin (increasing intracellular cAMP levels) activated the gluconeogenic program in HepG2 cells, a commonly used human hepatoma cell line (Figure 1M), in agreement with previous results (28). However, knockdown of *PRMT1* significantly ablated the response of HepG2 cells to glucagon plus forskolin stimulation (Figure 1M), confirming that the role of PRMT1 in glucose regulation is conserved in human liver cells.

PRMT1V2 plays a dominant role in activating the hepatic gluconeogenic program

Among the various isoforms of PRMT1, which one(s) may contribute primarily to this critical role in gluconeogenic regulation is completely unknown. We first investigated the relative expression of *Prmt1v1* and *Prmt1v2* in the liver, the two dominant isoforms in humans that differs from each other by a CRM1-dependent nuclear export sequence (Figure 2A) (16). We found that the expression of *Prmt1v2* was higher than *Prmt1v1* in the liver from WT mice (Supplementary Figure 4A). A similar expression pattern of *Prmt1v1* and *Prmt1v2* was observed in primary hepatocytes isolated from WT mice, Hepa 1-6 cells (a murine hepatoma cell line) and HepG2 cells (Supplementary Figure 4, B-D). Interestingly, western blot analyses of subcellular fractionations revealed that PRMT1 expression within the nucleus was increased in the fasted liver while cytosolic PRMT1 remained unchanged (Figure 2B), suggesting that PRMT1V2 might be the isoform that activates hepatic gluconeogenesis.

To further explore the role of these two isoforms in the hepatic glucose production, gain-of-function experiments were carried out with adenoviruses that overexpress PRMT1V1 and PRMT1V2, which displayed subcellular expression pattern as expected (Figure 2, C-G, Supplementary Figure 4, E-G). Overexpression of PRMT1V2 significantly induced the

expression of gluconeogenic genes in the mouse primary hepatocytes whereas little effects were observed in cells overexpressing PRMT1V1 (Figure 2, D and F).

To test this effect in vivo, we ectopically expressed PRMT1V1 and PRMT1V2 in the mice with hepatic deletion of endogenous *Prmt1* (Figure 2, H-J). Mice injected with adenovirus overexpressing PRMT1V2 displayed higher blood glucose levels after fasting for 6 and 16 hours (Figure 2K). However, there was no difference in fasted blood glucose levels between mice injected with adenovirus overexpressing GFP and PRMT1V1 (Figure 2K). In addition, gluconeogenic genes, including *Pck1*, *G6pc*, *Ppargc1a*, and *Cebpb*, were significantly induced in mice with PRMT1V2 overexpression, but not PRMT1V1, after 16-hour fasting (Figure 2L). PTT results demonstrated that hepatic gluconeogenic capacity was augmented in mice with PRMT1V2 overexpression but remained unchanged in mice with PRMT1V1 overexpression (Figure 2M). Similar to what was observed in murine primary hepatocytes, overexpression of PRMT1V1 did not affect the gluconeogenic program in HepG2 cells (Figure 2, N and O). On the contrary, PRMT1V2 overexpression significantly increased the expression of gluconeogenic genes (Figure 2, P and Q). These results suggest that PRMT1V2 plays a major role in regulating hepatic gluconeogenesis.

PRMT1V2 stimulates hepatic gluconeogenesis via PGC1α

PGC1α is a transcriptional coactivator that regulates multiple physiological functions in metabolism, including adaptive thermogenesis and gluconeogenesis (3, 4, 29). It has been reported that the arginine residues of PGC1α could be methylated by PRMT1 and its coactivator activity was increased after methylation (9). Consistent with previous reports (4), overexpression of PGC1α significantly induced the expression of gluconeogenic genes (Figure 3A). Co-overexpression of PRMT1V2 but not PRMT1V1 with PGC1α can lead to further increase in expression levels of gluconeogenic genes in primary hepatocytes, likely through activated PGC1α that was methylated primarily by nucleus-located PRMT1V2 but not PRMT1V1 in the cytosol (Figure 3, B and C). This gluconeogenic effect of PRMT1V2 was also observed in experiments testing *Pck1* promoter activity in Hepa 1-6 cells (Figure 3, D and E). In Hepa 1-6 cells, knockdown of *Ppargc1a* reduced *Pck1*-luciferase activity (Figure 3, F-H). Transient transfection of PRMT1V2 increased *Pck1*-luciferase activity while there were no effects observed in cells transfected with PRMT1V1 (Figure 3, G and H). Notably, knockdown of *Ppargc1a* completely abolished the stimulatory effects of PRMT1V2 (Figure 3H). This drastic effects of PGC1α on PRMT1V2 function in the hepatic gluconeogenic regulation were further revealed when PRMT1V1 and PRMT1V2 were individually re-introduced back in *Alb-Cre*;*Prmt1*$^{fl/fl}$ mice after knockdown of *Ppargc1a* (Figure 3, I-K). Elevated fasting blood glucose levels, induced gluconeogenic gene expression and compromised pyruvate tolerance observed previously with PRMT1V2 overexpression were completely blunted in the absence of PGC1α (Figure 3, I-K). Similar results were observed in vitro in the primary hepatocytes demonstrating a likely cell-autonomous mechanism (Supplementary Figure 5, A and B). Conversely, even though injection with the adenovirus encoding an shRNA specific to *Ppargc1a* decreased the gluconeogenic capacity as expected in the *Prmt1*$^{fl/fl}$ mice, knockdown of *Ppargc1a* did not render further reduction in gluconeogenesis in *Alb-Cre*;*Prmt1*$^{fl/fl}$ mice, demonstrating the

physiological significance of this PGC1α and PRMT1 interaction in vivo. (Supplementary Figure 5, C-E).

It has been reported that PRMT1 may regulate glucose production through FOXO1, a transcription factor known to activate gluconeogenesis in the liver (27, 30). But which isoform of PRMT1 may be involved in this process has not been investigated. In contrast to the dominant effects of PRMT1V2 when working with PGC1α, both PRMT1V1 and PRMT1V2 can further increase *Pck1*-luciferase activity when co-overexpressed with FOXO1 (Supplementary Figure 6, A and B). This coactivation between PRMT1 and FOXO1 remained functional in the cells infected with an adenovirus encoding an shRNA specific to *Ppargc1a* (Supplementary Figure 6, C and D), suggesting that PRMT1 may regulate hepatic gluconeogenesis with different partners through various mechanisms.

We next explored whether PRMT1V2 functions with PGC1α in hepatic gluconeogenic regulation in human liver cells. Similar to what we observed in murine hepatocytes, co-overexpression of PRMT1V2 and PGC1α further increased gluconeogenic gene expression and *Pck1* promoter activity compared with those observed in cells only ectopically overexpressing PGC1α, whereas little effects were observed with PRMT1V1 (Figure 3, L-O).

Further mechanistic investigation was carried out to test whether PRMT1V2 enhances PGC1α activity through arginine methylation. In contrast to what was observed with the wild-type PRMT1V2, which increased *Pck1*-luciferase activity when co-overexpressed with PGC1α, PRMT1V2-G98R, a catalytically inactive mutant (Figure 4, A and B) (19, 20), did not show any synergistic effects with PGC1α mediating *Pck1* promoter activation (Figure 4C). It has been proposed that the potential methylation sites of PRMT1 on PGC1α, arginine residues 665, 667, and 669, locate within the C-terminal E region (9). Even though when expressed alone, either a mutant PGC1α-ΔE without E region or a mutant PGC1α-R3K consisting of conversion of arginine residues 665, 667, and 669 to lysine can increase *Pck1*-luciferase activity, neither mutant demonstrated coactivation effects when co-expressed with PRMT1V2 (Figure 4, D-H). These results collectively support the hypothesis that PRMT1V2 mediates PGC1α function primarily through arginine methylation.

Our results demonstrated that PRMT1, variant 2 in particular, modulated hepatic gluconeogenesis via PGC1α. We next tested, as the master regulator of gluconeogenesis, whether PGC1α regulates PRMT1 expression in hepatocytes. PGC1α overexpression in HepG2 cells did not lead to changes in *PRMT1* mRNA levels (Figure 4I), whereas increased protein levels of PRMT1 were detected in cells with adenovirus overexpressing PGC1α (Figure 4J). It has been reported that PRMT1 protein can be stabilized through downregulation of p300 (EP300) and Sirtuin 1 (Sirt1) (22). Indeed, overexpression of PGC1α led to decreased expression of *EP300* and *SIRT1* in HepG2 cells (Figure 4K). Furthermore, glucagon treatments no longer stabilized PRMT1 in the hepatocytes in the absence of PGC1α (Figure 4L). These results collectively suggest that as a part of the machinery of glucose control in the liver, PRMT1 itself is regulated by PGC1α, which forms a feedback regulatory loop.

Liver-specific *Prmt1* deficiency counteracts diabetic hyperglycemia

Excessive hepatic gluconeogenesis and loss of glycemic control is one of the characteristics of diabetes and metabolic syndrome (1, 31, 32). Whether PRMT1 modulates pathological hepatic glucose production in diabetes may be of great clinical relevance. Streptozocin (STZ) is widely used to kill insulin-producing beta cells, causes acute glucotoxicity effects in vivo and induces type 1 diabetes in mice (33). Mice injected with STZ displayed higher fed blood glucose levels when compared with mice injected with vehicle (Figure 5A). In this type 1 diabetes mouse model, *Prmt1* was markedly increased along with the induction of gluconeogenic genes (Figure 5, A and B). It is of note that *Prmt1v1* was not changed but *Prmt1v2* was significantly induced in the liver of mice injected with STZ (Figure 5A). These results suggest that PRMT1 is involved in the inappropriate hepatic glucose production in diabetes.

To investigate how the absence of *Prmt1* may affect pathological hepatic gluconeogenesis, we injected *Alb-Cre*;*Prmt1*$^{fl/fl}$ and *Prmt1*$^{fl/fl}$ control mice with STZ. After STZ injection, liver-specific deletion of *Prmt1* resulted in less elevated blood glucose levels and less induced gluconeogenic gene expression in the liver in the fed state compared to STZ-injected *Prmt1*$^{fl/fl}$ control mice (Figure 5, C and D). GTT revealed that *Alb-Cre*;*Prmt1*$^{fl/fl}$ mice had better control of glycemia after STZ injection (Figure 5E). These results indicate that hepatic deletion of *Prmt1* may protect against pathological hepatic gluconeogenesis in type 1 diabetes.

In addition to type 1 diabetes, hepatic regulation of glucose constitutes a very important aspect of liver dysfunction in various metabolic disorders. Chronic HFD feeding promotes obesity and insulin resistance and has been used as a model to induce both type 2 diabetes and nonalcoholic fatty liver disease (NAFLD) in mice (34). Mice on HFD had higher body weights and elevated fasting blood glucose levels compared with mice on chow diet as expected (Figure 5F). qPCR analyses showed that *Prmt1* was significantly induced in the liver by HFD feeding, accompanied by the activation of gluconeogenic genes, including *Pck1*, *G6pc*, and *Cebpb* (Figure 5, G and H). In particular, *Prmt1v2* was significantly increased in the liver from mice on HFD while there was no difference in the expression of *Prmt1v1* between mice on chow diet and HFD (Figure 5G).

Similar to what was observed in STZ-induced type 1 diabetes model, when challenged with HFD feeding, hepatic deletion of *Prmt1* provided protection against hyperglycemia in this type 2 diabetes model. Upon HFD feeding, *Alb-Cre*;*Prmt1*$^{fl/fl}$ mice showed lower body weight gain and less liver tissue mass than those of the littermate control animals without differences in food intake (Figure 5, I and J, Supplementary Figure 7A). After fasting, blood glucose was lower and gluconeogenic genes were less induced in the liver in *Alb-Cre*;*Prmt1*$^{fl/fl}$ than those of controls (Figure 5, K and L). *Alb-Cre*;*Prmt1*$^{fl/fl}$ mice on HFD showed less impaired glucose tolerance compared to littermate control while these two genotypes showed comparable glycemia control on chow diet (Figure 5M, Supplementary Figure 7B). Together, these data indicate that inhibiting hepatic PRMT1 activity may protect against inappropriate glucose production due to insulin resistance.

In comparison to standard HFD, so called western diets, which contains high-fat, high fructose and high cholesterol, are more widely used as a more specific model for fatty liver study, which better mimics fast food style diets (34). It is of great interest to observe that *Prmt*1, particularly *Prmt1v2* was increased in the livers of mice challenged with western diet and loss of hepatic *Prmt1* protected mice from metabolic dysfunction caused by a western diet (Supplementary Figure 8). These data indicate that PRMT1 may be involved in hepatic regulation in a broad spectrum of metabolic disorders.

Discussion

Our study revealed that *Prmt1* deficiency results in impaired gluconeogenesis in the liver during fasting. PRMT1V2 is the isoform that is primarily responsible for glucose regulation through interactions with PGC1α and this mechanism is conserved in human hepatocytes. Hepatic deletion of *Prmt1* protects against inappropriate activation of gluconeogenesis in metabolic disorder, such as diabetes.

The expression profiling of different isoforms of *Prmt1* showed that *Prmt1v2* was expressed at a higher level than *Prmt1v1* in mouse and human hepatocytes. Functional analyses revealed that PRMT1V2 activated the gluconeogenic program in the hepatocytes and augmented glucose production in vivo, while there were no effects of PRMT1V1. The difference between *Prmt1v1* and *Prmt1v2* is that there is a nuclear export sequence in *Prmt1v1* which makes PRMT1V1 exported to the cytoplasm and PRMT1V2 exist in the nucleus (16) (Figure 2, A and C), indicating that PRMT1V2 may activate gluconeogenesis through modulating transcription, likely through controlling methylation of transcriptional regulators, such as PGC1α (Figure 3C, Figure 4, A-H).

A previous study has implicated that PRMT1 may be involved in glucose control through a FOXO1-dependent mechanism (27). However, the differential regulation via different isoforms of PRMT1 was not investigated. It is also of note that the levels of PRMT1 protein were significantly reduced in the $Prmt1^{+/-}$ mice in this previous study (27), whereas similar protein levels of PRMT1 were detected in the liver of *Alb-Cre*;$Prmt1^{fl/+}$ mice compared to that in the control $Prmt1^{fl/fl}$ mice in our study. It is conceivable that systemic haploinsufficiency of PRMT1 may lead to secondary influence on liver function and complicate the interpretation of the phenotype observed in $Prmt1^{+/-}$ mice. We observed that, when co-overexpressed, both PRMT1V1 and PRMT1V2 works with FOXO1 to activates *Pck1* promoter activity regardless the presence or absence of PGC1α, indicating that PRMT1 closely interacts with key modulators of liver glucose control through multiple mechanisms.

Our study revealed a feedback regulation between PRMT1V2 and PGC1α in hepatocytes. PGC1α was strongly induced in the liver of mice in the fasted state and overexpression of PGC1α through adenoviral delivery stimulated hepatic gluconeogenesis (4). Deletion of *Ppargc1a* reduced the hepatic glucose production in the fasted mice (29). It has been reported that PGC1α is induced in STZ-induced and *db*/*db* diabetic mice (4, 35). Knockdown of *Ppargc1a* could reduce hepatic gluconeogenesis in the diabetes mouse model (35). Intriguingly, it is also well documented that *PPARGC1A* expression is reduced in

the liver of humans with diabetes and NAFLD (36-38). The precise modulation of PGC1α activity in the liver is critical in systemic glucose control (39). Our study suggests that PRMT1V2 represents another key module in this complex network that acutely senses nutritional and hormonal cues and consists of many regulators, including PGC1α and FOXO1.

Protein arginine methylation is an important posttranscriptional modification for protein function (40). It has been reported that multiple cellular processes are regulated by arginine methylation, including RNA processing, signaling transduction, and transcriptional regulation (40). PRMT1 is the key member of the PRMT family, which is responsible for most of the asymmetric dimethylation. PRMT1 is expressed in various tissues (25). It has been reported that PRMT1 is involved in a variety of biological processes, including transcriptional control, DNA repair, mRNA splicing, and signal transduction (10). PRMT1 was further shown to play a role in cancer progression (41) and thermogenesis activation in fat (15). Previous studies indicated that PRMT1 regulates lipogenesis in hepatic steatosis and alcohol-induced liver dysfunction (14, 26, 42-44). Despite of the fact that pleiotropic effects of PRMT1 have been investigated in various tissues, the unique discovery of the current study lies in the specific and finetuned regulation mediated by this interaction between PGC1α and PRMT1V2. This isoform specific coactivation is regulated primarily by nucleus localized PRMT1V2. On the one hand, methylation-resistant form of PGC1α can still regulate gluconeogenesis (Figure 4, E and G), suggesting, not surprisingly, this master regulator of liver function can be modulated by other factors besides PRMT1. Yet, the synergistic effects between PGC1α and PRMT1V2 are almost completely absent when arginine methylation is blocked. Either loss of catalytical ability of PRMT1V2 or mutations in the potential arginine methylation sites in PGC1α abolished the synergistic effects of this PGC1α and PRMT1 interaction. PGC1α is mechanistically involved in the glucagon mediated stabilization of PRMT1V2 on the protein level, whereas, the other hormone crucial in glycemic control, insulin, posts minimal effects in this process. The specificity at each step of this pathway may prove to be advantageous when aiming for targeted effects in future efforts strategizing therapeutic intervention against pathological hyperglycemia.

Lastly, our study revealed impressive functional significance of this interaction. With deletion of *Prmt1* in hepatocytes, mice displayed better glycemia control and overall improved metabolic health when challenged with STZ injection or HFD feeding, indicating that PRMT1 played a critical role in the regulation of inappropriate hepatic glucose production in diabetes. Given that *PRMT1V2* was significantly induced in the liver of multiple metabolic disease settings where liver dysfunction is involved, ongoing drug development efforts to identify specific inhibitor for PRMT1 may be of great therapeutic potential in the near future (45).

Supplementary Material

Refer to Web version on PubMed Central for supplementary material.

Acknowledgements

This work was supported by a grant from the American Diabetes Association (1-18-IBS-281 to JWu) and AGA-Allergan Foundation pilot research award from the American Gastroenterological Association (AGA2020-21-09 to JWu), and fellowships from the Chinese Scholarship Council (201806370290 to YM, 201908420207 to JWang). We thank Dr. Michael Stallcup at the University of Southern California for sharing plasmids expressing PGC1α-ΔE and PGC1α-R3K.

Abbreviations:

cAMP	Cyclic adenosine monophosphate
CHX	Cycloheximide
CRM1	Chromosome region maintenance 1/exportin1/Exp1/Xpo1
GAN	Gubra Amylin NASH
GTT	Glucose tolerance test
HFD	High fat diet
NASH	Nonalcoholic steatohepatitis
PRMT	Protein arginine methyltransferase
PTT	Pyruvate tolerance test
STZ	Streptozocin

References

1. Rines AK, Sharabi K, Tavares CD, and Puigserver P (2016) Targeting hepatic glucose metabolism in the treatment of type 2 diabetes. Nat Rev Drug Discov 15, 786–804 [PubMed: 27516169]
2. Rui L (2014) Energy metabolism in the liver. Compr Physiol 4, 177–197 [PubMed: 24692138]
3. Puigserver P, Wu Z, Park CW, Graves R, Wright M, and Spiegelman BM (1998) A cold-inducible coactivator of nuclear receptors linked to adaptive thermogenesis. Cell 92, 829–839 [PubMed: 9529258]
4. Yoon JC, Puigserver P, Chen G, Donovan J, Wu Z, Rhee J, Adelmant G, Stafford J, Kahn CR, Granner DK, Newgard CB, and Spiegelman BM (2001) Control of hepatic gluconeogenesis through the transcriptional coactivator PGC-1. Nature 413, 131–138 [PubMed: 11557972]
5. Rhee J, Inoue Y, Yoon JC, Puigserver P, Fan M, Gonzalez FJ, and Spiegelman BM (2003) Regulation of hepatic fasting response by PPARgamma coactivator-1alpha (PGC-1): requirement for hepatocyte nuclear factor 4alpha in gluconeogenesis. Proc Natl Acad Sci U S A 100, 4012–4017 [PubMed: 12651943]
6. Rodgers JT, Lerin C, Haas W, Gygi SP, Spiegelman BM, and Puigserver P (2005) Nutrient control of glucose homeostasis through a complex of PGC-1alpha and SIRT1. Nature 434, 113–118 [PubMed: 15744310]
7. Puigserver P, Rhee J, Donovan J, Walkey CJ, Yoon JC, Oriente F, Kitamura Y, Altomonte J, Dong H, Accili D, and Spiegelman BM (2003) Insulin-regulated hepatic gluconeogenesis through FOXO1-PGC-1alpha interaction. Nature 423, 550–555 [PubMed: 12754525]
8. Lin J, Handschin C, and Spiegelman BM (2005) Metabolic control through the PGC-1 family of transcription coactivators. Cell Metab 1, 361–370 [PubMed: 16054085]
9. Teyssier C, Ma H, Emter R, Kralli A, and Stallcup MR (2005) Activation of nuclear receptor coactivator PGC-1alpha by arginine methylation. Genes Dev 19, 1466–1473 [PubMed: 15964996]

10. Bedford MT, and Clarke SG (2009) Protein arginine methylation in mammals: who, what, and why. Mol Cell 33, 1–13 [PubMed: 19150423]
11. Blanc RS, and Richard S (2017) Arginine Methylation: The Coming of Age. Mol Cell 65, 8–24 [PubMed: 28061334]
12. Iwasaki H, and Yada T (2007) Protein arginine methylation regulates insulin signaling in L6 skeletal muscle cells. Biochem Biophys Res Commun 364, 1015–1021 [PubMed: 17971302]
13. Pyun JH, Kim HJ, Jeong MH, Ahn BY, Vuong TA, Lee DI, Choi S, Koo SH, Cho H, and Kang JS (2018) Cardiac specific PRMT1 ablation causes heart failure through CaMKII dysregulation. Nat Commun 9, 5107 [PubMed: 30504773]
14. Park MJ, Kim DI, Lim SK, Choi JH, Kim JC, Yoon KC, Lee JB, Lee JH, Han HJ, Choi IP, Kim HC, and Park SH (2014) Thioredoxin-interacting protein mediates hepatic lipogenesis and inflammation via PRMT1 and PGC-1alpha regulation in vitro and in vivo. J Hepatol 61, 1151–1157 [PubMed: 25003952]
15. Qiao X, Kim DI, Jun H, Ma Y, Knights AJ, Park MJ, Zhu K, Lipinski JH, Liao J, Li Y, Richard S, Weinman SA, and Wu J (2019) Protein Arginine Methyltransferase 1 Interacts With PGC1alpha and Modulates Thermogenic Fat Activation. Endocrinology 160, 2773–2786 [PubMed: 31555811]
16. Goulet I, Gauvin G, Boisvenue S, and Cote J (2007) Alternative splicing yields protein arginine methyltransferase 1 isoforms with distinct activity, substrate specificity, and subcellular localization. J Biol Chem 282, 33009–33021 [PubMed: 17848568]
17. Tikhanovich I, Zhao J, Olson J, Adams A, Taylor R, Bridges B, Marshall L, Roberts B, and Weinman SA (2017) Protein arginine methyltransferase 1 modulates innate immune responses through regulation of peroxisome proliferator-activated receptor gamma-dependent macrophage differentiation. J Biol Chem 292, 6882–6894 [PubMed: 28330868]
18. Wu J, Ruas JL, Estall JL, Rasbach KA, Choi JH, Ye L, Bostrom P, Tyra HM, Crawford RW, Campbell KP, Rutkowski DT, Kaufman RJ, and Spiegelman BM (2011) The unfolded protein response mediates adaptation to exercise in skeletal muscle through a PGC-1alpha/ATF6alpha complex. Cell Metab 13, 160–169 [PubMed: 21284983]
19. Liu X, Li H, Liu L, Lu Y, Gao Y, Geng P, Li X, Huang B, Zhang Y, and Lu J (2016) Methylation of arginine by PRMT1 regulates Nrf2 transcriptional activity during the antioxidative response. Biochim Biophys Acta 1863, 2093–2103 [PubMed: 27183873]
20. Sakamaki J, Daitoku H, Ueno K, Hagiwara A, Yamagata K, and Fukamizu A (2011) Arginine methylation of BCL-2 antagonist of cell death (BAD) counteracts its phosphorylation and inactivation by Akt. Proc Natl Acad Sci U S A 108, 6085–6090 [PubMed: 21444773]
21. Tong X, Zhang D, Charney N, Jin E, VanDommelen K, Stamper K, Gupta N, Saldate J, and Yin L (2017) DDB1-Mediated CRY1 Degradation Promotes FOXO1-Driven Gluconeogenesis in Liver. Diabetes 66, 2571–2582 [PubMed: 28790135]
22. Lai Y, Li J, Li X, and Zou C (2017) Lipopolysaccharide modulates p300 and Sirt1 to promote PRMT1 stability via an SCF(Fbxl17)-recognized acetyldegron. J Cell Sci 130, 3578–3587 [PubMed: 28883095]
23. Qiu K, Liang W, Wang S, Kong T, Wang X, Li C, Wang Z, and Wu Y (2020) BACE2 degradation is mediated by both the proteasome and lysosome pathways. BMC Mol Cell Biol 21, 13 [PubMed: 32160867]
24. Hatting M, Tavares CDJ, Sharabi K, Rines AK, and Puigserver P (2018) Insulin regulation of gluconeogenesis. Ann N Y Acad Sci 1411, 21–35 [PubMed: 28868790]
25. Tang J, Frankel A, Cook RJ, Kim S, Paik WK, Williams KR, Clarke S, and Herschman HR (2000) PRMT1 is the predominant type I protein arginine methyltransferase in mammalian cells. J Biol Chem 275, 7723–7730 [PubMed: 10713084]
26. Zhao J, Adams A, Weinman SA, and Tikhanovich I (2019) Hepatocyte PRMT1 protects from alcohol induced liver injury by modulating oxidative stress responses. Sci Rep 9, 9111 [PubMed: 31235809]
27. Choi D, Oh KJ, Han HS, Yoon YS, Jung CY, Kim ST, and Koo SH (2012) Protein arginine methyltransferase 1 regulates hepatic glucose production in a FoxO1-dependent manner. Hepatology 56, 1546–1556 [PubMed: 22532369]

28. Jackson MI, Cao J, Zeng H, Uthus E, and Combs GF Jr. (2012) S-adenosylmethionine-dependent protein methylation is required for expression of selenoprotein P and gluconeogenic enzymes in HepG2 human hepatocytes. J Biol Chem 287, 36455–36464 [PubMed: 22932905]
29. Lin J, Wu PH, Tarr PT, Lindenberg KS, St-Pierre J, Zhang CY, Mootha VK, Jager S, Vianna CR, Reznick RM, Cui L, Manieri M, Donovan MX, Wu Z, Cooper MP, Fan MC, Rohas LM, Zavacki AM, Cinti S, Shulman GI, Lowell BB, Krainc D, and Spiegelman BM (2004) Defects in adaptive energy metabolism with CNS-linked hyperactivity in PGC-1alpha null mice. Cell 119, 121–135 [PubMed: 15454086]
30. Matsumoto M, Pocai A, Rossetti L, Depinho RA, and Accili D (2007) Impaired regulation of hepatic glucose production in mice lacking the forkhead transcription factor Foxo1 in liver. Cell Metab 6, 208–216 [PubMed: 17767907]
31. Priya G, and Kalra S (2018) A Review of Insulin Resistance in Type 1 Diabetes: Is There a Place for Adjunctive Metformin? Diabetes Ther 9, 349–361 [PubMed: 29139080]
32. Gastaldelli A, and Cusi K (2019) From NASH to diabetes and from diabetes to NASH: Mechanisms and treatment options. JHEP Rep 1, 312–328 [PubMed: 32039382]
33. Wu J, and Yan LJ (2015) Streptozotocin-induced type 1 diabetes in rodents as a model for studying mitochondrial mechanisms of diabetic beta cell glucotoxicity. Diabetes Metab Syndr Obes 8, 181–188 [PubMed: 25897251]
34. Van Herck MA, Vonghia L, and Francque SM (2017) Animal Models of Nonalcoholic Fatty Liver Disease-A Starter's Guide. Nutrients 9
35. Koo SH, Satoh H, Herzig S, Lee CH, Hedrick S, Kulkarni R, Evans RM, Olefsky J, and Montminy M (2004) PGC-1 promotes insulin resistance in liver through PPAR-alpha-dependent induction of TRB-3. Nat Med 10, 530–534 [PubMed: 15107844]
36. Ahrens M, Ammerpohl O, von Schonfels W, Kolarova J, Bens S, Itzel T, Teufel A, Herrmann A, Brosch M, Hinrichsen H, Erhart W, Egberts J, Sipos B, Schreiber S, Hasler R, Stickel F, Becker T, Krawczak M, Rocken C, Siebert R, Schafmayer C, and Hampe J (2013) DNA methylation analysis in nonalcoholic fatty liver disease suggests distinct disease-specific and remodeling signatures after bariatric surgery. Cell Metab 18, 296–302 [PubMed: 23931760]
37. Koliaki C, Szendroedi J, Kaul K, Jelenik T, Nowotny P, Jankowiak F, Herder C, Carstensen M, Krausch M, Knoefel WT, Schlensak M, and Roden M (2015) Adaptation of hepatic mitochondrial function in humans with non-alcoholic fatty liver is lost in steatohepatitis. Cell Metab 21, 739–746 [PubMed: 25955209]
38. Westerbacka J, Kolak M, Kiviluoto T, Arkkila P, Siren J, Hamsten A, Fisher RM, and Yki-Jarvinen H (2007) Genes involved in fatty acid partitioning and binding, lipolysis, monocyte/macrophage recruitment, and inflammation are overexpressed in the human fatty liver of insulin-resistant subjects. Diabetes 56, 2759–2765 [PubMed: 17704301]
39. Besse-Patin A, Jeromson S, Levesque-Damphousse P, Secco B, Laplante M, and Estall JL (2019) PGC1A regulates the IRS1:IRS2 ratio during fasting to influence hepatic metabolism downstream of insulin. Proc Natl Acad Sci U S A 116, 4285–4290 [PubMed: 30770439]
40. Bedford MT, and Richard S (2005) Arginine methylation an emerging regulator of protein function. Mol Cell 18, 263–272 [PubMed: 15866169]
41. Yang Y, and Bedford MT (2013) Protein arginine methyltransferases and cancer. Nat Rev Cancer 13, 37–50 [PubMed: 23235912]
42. Zhao J, Adams A, Roberts B, O'Neil M, Vittal A, Schmitt T, Kumer S, Cox J, Li Z, Weinman SA, and Tikhanovich I (2018) Protein arginine methyl transferase 1- and Jumonji C domain-containing protein 6-dependent arginine methylation regulate hepatocyte nuclear factor 4 alpha expression and hepatocyte proliferation in mice. Hepatology 67, 1109–1126 [PubMed: 29023917]
43. Zhang XP, Jiang YB, Zhong CQ, Ma N, Zhang EB, Zhang F, Li JJ, Deng YZ, Wang K, Xie D, and Cheng SQ (2018) PRMT1 Promoted HCC Growth and Metastasis In Vitro and In Vivo via Activating the STAT3 Signalling Pathway. Cell Physiol Biochem 47, 1643–1654 [PubMed: 29945155]
44. Zhao J, O'Neil M, Vittal A, Weinman SA, and Tikhanovich I (2019) PRMT1-Dependent Macrophage IL-6 Production Is Required for Alcohol-Induced HCC Progression. Gene Expr 19, 137–150 [PubMed: 30236171]

45. Sun Y, Wang Z, Yang H, Zhu X, Wu H, Ma L, Xu F, Hong W, and Wang H (2019) The Development of Tetrazole Derivatives as Protein Arginine Methyltransferase I (PRMT I) Inhibitors. Int J Mol Sci 20

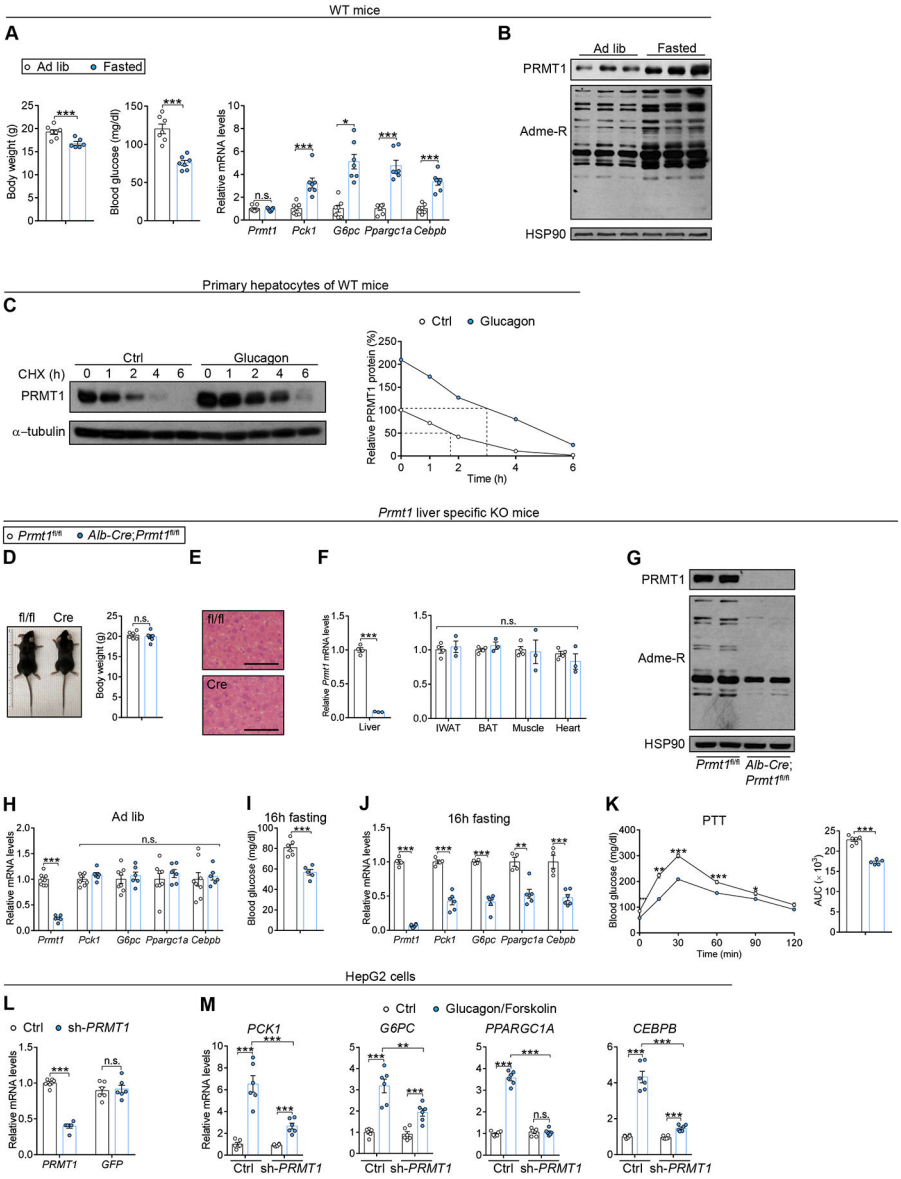

Figure 1.

Loss of *Prmt1* reduces gluconeogenic capacity in the liver. *A*) Body weights (left; n = 7 for ad lib, n = 6 for fasted), blood glucose levels (middle; n = 7/group), and qPCR analyses (right; n = 7/group) of *Prmt1* and gluconeogenic marker mRNA levels in the liver of wild-type (WT) mice under ad libitum-fed and 16 hour-fasted conditions. *B*) Immunoblot analyses of PRMT1 and asymmetric-dimethylated arginine (Adme-R) in the liver of mice described in (*A*) (n = 3/group). HSP90 was used as a loading control. *C*) Immunoblot (left) and quantification (right) analyses of PRMT1 in the primary hepatocytes isolated from WT mice and treated with 100 μg/mL cycloheximide (CHX) for indicated time after pretreatment with vehicle (Ctrl) or 200 nM glucagon for 3 hours. α-tubulin was used as a loading control. *D*) Body weights of *Prmt1*$^{fl/fl}$ and *Alb-Cre*;*Prmt1*$^{fl/fl}$ mice under basal conditions (chow diet, fed state, n = 6/group). *E*) H&E-stained images of the liver in mice described in (*D*) (scale bar, 100 μm). *F*) qPCR analyses of *Prmt1* mRNA levels across tissues from *Prmt1*$^{fl/fl}$ and

Alb-Cre;*Prmt1*$^{fl/fl}$ mice (n = 4 for *Prmt1*$^{fl/fl}$, n = 3 for *Alb-Cre*;*Prmt1*$^{fl/fl}$). *G*) Immunoblot analyses of PRMT1 and Adme-R in the liver from mice described in (*D*) (n = 2/group). HSP90 was used as a loading control. *H*) qPCR analyses of *Prmt1* and gluconeogenic marker mRNA levels in *Prmt1*$^{fl/fl}$ and *Alb-Cre*;*Prmt1*$^{fl/fl}$ mice under basal conditions (chow diet; fed state; n = 8 for *Prmt1*$^{fl/fl}$, n = 6 for *Alb-Cre*;*Prmt1*$^{fl/fl}$). *I*) Blood glucose levels of 16 hour-fasted *Prmt1*$^{fl/fl}$ and *Alb-Cre*;*Prmt1*$^{fl/fl}$ mice (n = 6 for *Prmt1*$^{fl/fl}$, n = 5 for *Alb-Cre*;*Prmt1*$^{fl/fl}$). *J*) qPCR analyses of *Prmt1* and gluconeogenic marker mRNA levels in the liver of mice described in (*I*) (n = 4 for *Prmt1*$^{fl/fl}$, n = 6 for *Alb-Cre*;*Prmt1*$^{fl/fl}$). *K*) PTT in 16 hour-fasted mice described in (*I*) (n = 6 for *Prmt1*$^{fl/fl}$, n = 5 for *Alb-Cre*;*Prmt1*$^{fl/fl}$). AUC, area under the curve. *L*) qPCR analyses of *PRMT1* and *GFP* mRNA levels in HepG2 cells infected with indicated adenoviruses (n = 6/group). *M*) qPCR analyses of gluconeogenic marker mRNA levels in HepG2 cells infected with indicated adenoviruses and stimulated with 1 mM glucagon plus 10 μM forskolin or vehicle (Ctrl) for 24 hours (n = 6/group). Data are presented as mean ± SEM. *$P < 0.05$; **$P < 0.01$; ***$P < 0.001$. n.s., not significant. 2-tailed Student's *t* test (A, D, F, H-L) or 2-way ANOVA (M).

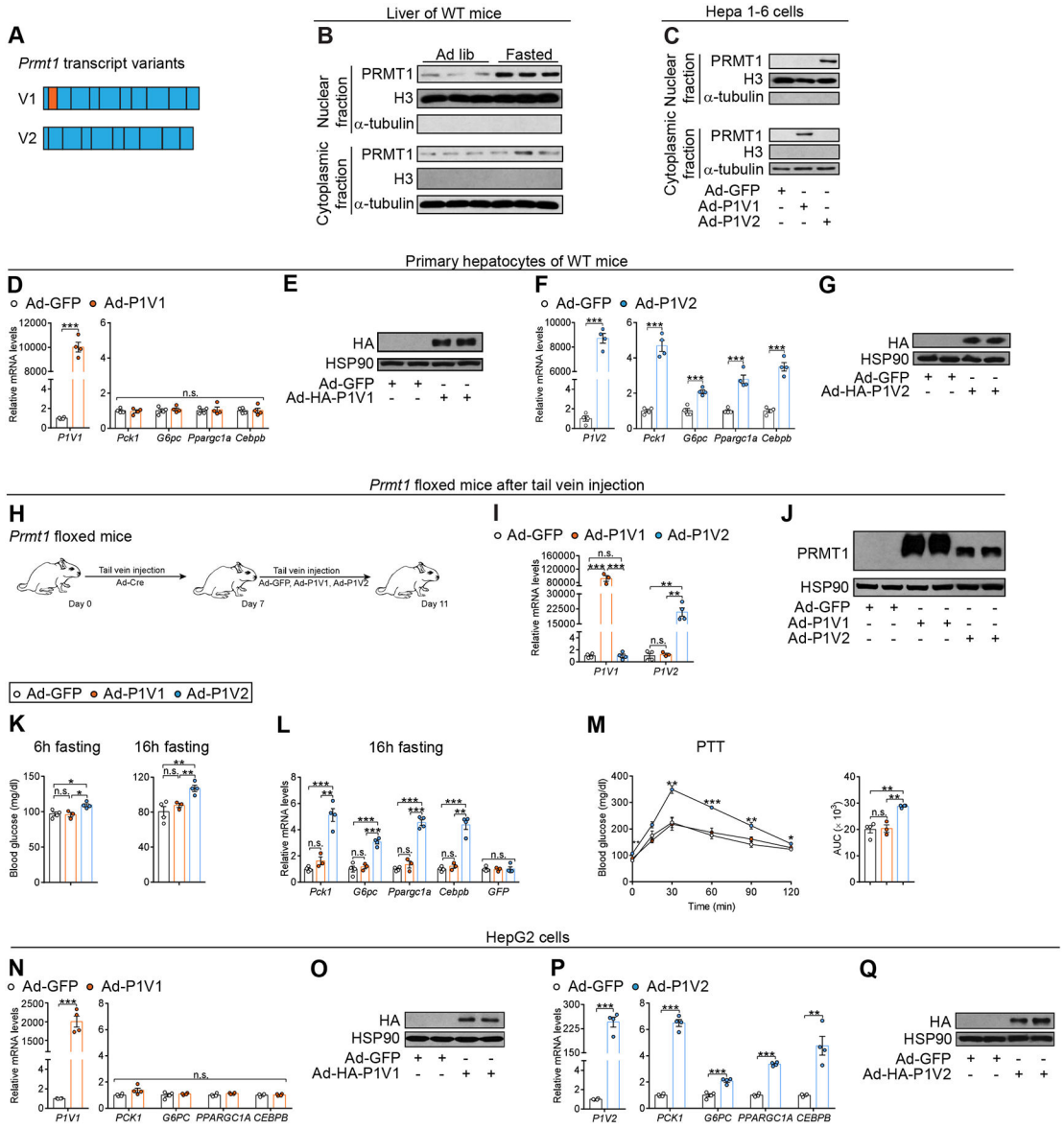

Figure 2.

PRMT1V2 (P1V2) is primarily responsible for the modulation of hepatic gluconeogenesis. *A*) Schematic of *PRMT1V1 (P1V1*) and *P1V2* transcript structure. *B*) Immunoblot analyses of PRMT1 in purified nuclear and cytoplasmic fractions of liver from wild-type (WT) mice under ad libitum-fed and 16 hour-fasted conditions. Histone H3 (H3) and α-tubulin served as nuclear and cytoplasmic markers, respectively. *C*) Immunoblot analyses of PRMT1 in purified nuclear and cytoplasmic fractions of Hepa 1-6 cells infected with indicated adenoviruses. Histone H3 (H3) and α-tubulin served as nuclear and cytoplasmic markers, respectively. *D*) qPCR analyses of *P1V1* and gluconeogenic marker mRNA levels after infection with indicated adenoviruses in primary hepatocytes isolated from WT mice (n = 4/group). *E*) Immunoblot analyses of HA-P1V1 with anti-HA antibody in primary hepatocytes described in (*D*) (n = 2/group). HSP90 was used as a loading control. *F*) qPCR analyses of *P1V2* and gluconeogenic marker mRNA levels after infection with indicated adenoviruses

in primary hepatocytes isolated from WT mice (n = 4/group). *G*) Immunoblot analyses of HA-P1V2 with anti-HA antibody in primary hepatocytes described in (*F*) (n = 2/group). HSP90 was used as a loading control. *H*) Schematic of the experiment. *Prmt1*$^{fl/fl}$ mice were injected with indicated adenovirus through tail vein for CRE-mediated deletion. Seven days after first injection, the mice were injected with indicated adenoviruses through tail vein for gain-of-function. *I*) qPCR analyses of *P1V1* and *P1V2* mRNA levels in the liver of 16 hour-fasted mice described in (*H*) (n = 4 for Ad-GFP and Ad-P1V2, n = 3 for Ad-P1V1). *J*) Immunoblot analyses of PRMT1 in the liver from mice described in (*H*) (n = 2/group). HSP90 was used as a loading control. *K*) Blood glucose levels in 6 hour- or 16 hour-fasted mice described in (*H*) (n = 4 for Ad-GFP and Ad-P1V2, n = 3 for Ad-P1V1). *L*) qPCR analyses of gluconeogenic markers and *GFP* mRNA levels in 16 hour-fasted mice described in (*H*) (n = 4 for Ad-GFP and Ad-P1V2, n = 3 for Ad-P1V1). *M*) PTT in 16 hour-fasted mice described in (*H*) (n = 4 for Ad-GFP and Ad-P1V2, n = 3 for Ad-P1V1). AUC, area under the curve. *N*) qPCR analyses of *P1V1* and gluconeogenic marker mRNA levels in HepG2 cells infected with indicated adenoviruses (n = 4/group). *O*) Immunoblot analyses of HA-P1V1 with anti-HA antibody in HepG2 cells described in (*N*) (n = 2/group). HSP90 was used as a loading control. *P*) qPCR analyses of *P1V2* and gluconeogenic marker mRNA levels in HepG2 cells infected with indicated adenoviruses (n = 4/group). *Q*) Immunoblot analyses of HA-P1V2 with anti-HA antibody in HepG2 cells described in (*P*) (n = 2/group). HSP90 was used as a loading control. Data are presented as mean ± SEM. **P* < 0.05; ***P* < 0.01; ****P* < 0.001. n.s., not significant. 2-tailed Student's *t* test (D, F, N, P) or 1-way ANOVA (I, K-M).

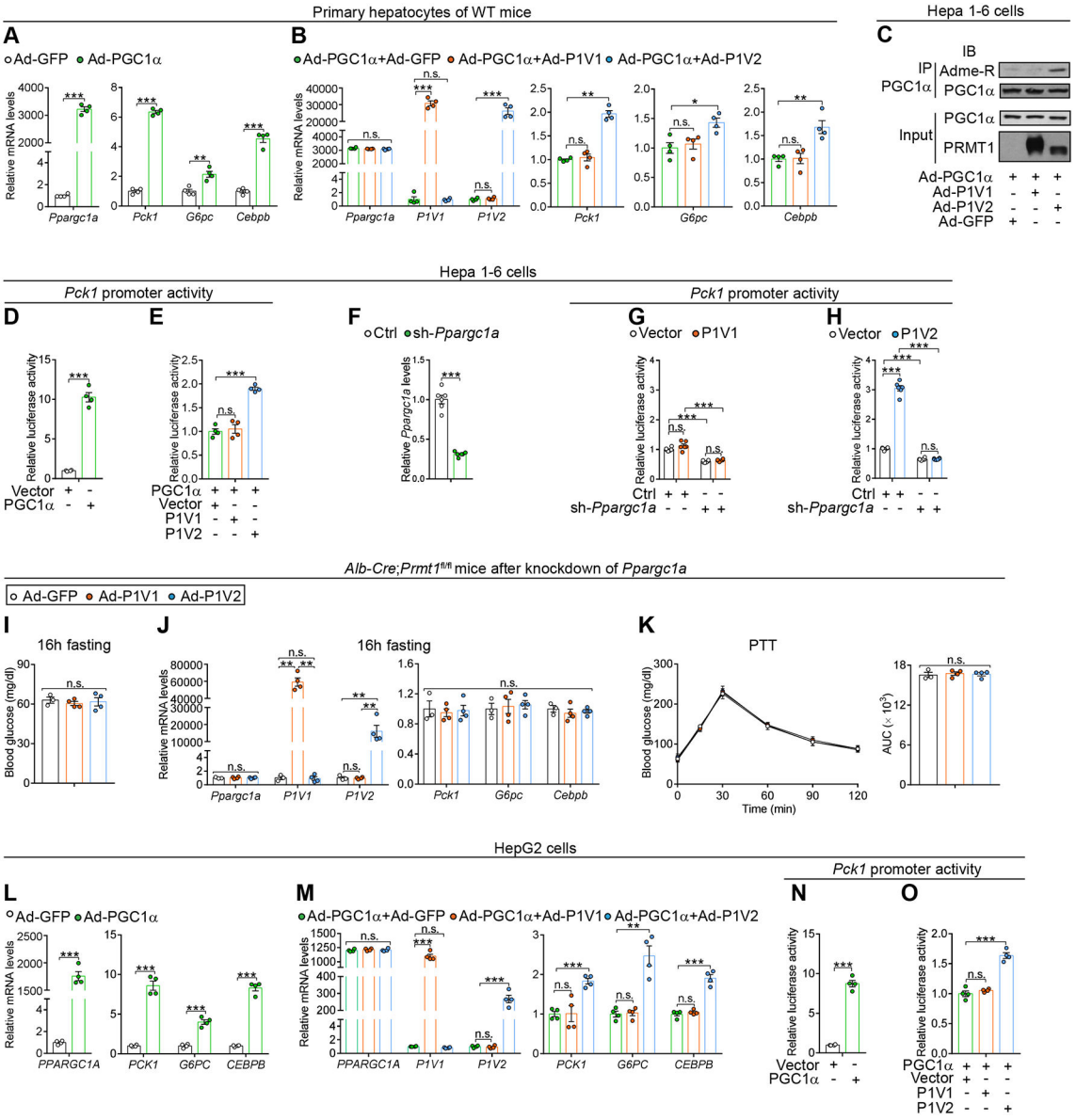

Figure 3.

PRMT1V2 activates hepatic gluconeogenesis through PGC1α. *A*) qPCR analyses of *Ppargc1a* and gluconeogenic marker mRNA levels in primary hepatocytes isolated from wild-type (WT) mice and infected with indicated adenoviruses (n = 4/group). *B*) qPCR analyses of *Ppargc1a, P1V1*, *P1V2*, and gluconeogenic marker mRNA levels in primary hepatocytes isolated from WT mice and infected with indicated adenoviruses (n = 4/group). *C*) Analyses of asymmetric dimethylation of PGC1α. Hepa 1-6 cells were infected with indicated adenoviruses. Lysates were immunoprecipitated with an anti-PGC1α antibody. Both input and immunoprecipitates were analyzed by immunoblotting as indicated. *D*, *E*) *Pck1* promoter activity in Hepa 1-6 cells transiently transfected with indicated vectors (n = 4/group). *F*) qPCR analyses of *Ppargc1a* mRNA levels in Hepa 1-6 cells infected with indicated adenoviruses (n = 6/group). *G*, *H*) *Pck1* promoter activity in Hepa 1-6 cells infected with indicated adenoviruses and then transiently transfected with indicated vectors

(n = 6/group). *I*) *Alb-Cre*;*Prmt1*$^{fl/fl}$ mice were first injected with the adenovirus encoding an shRNA specific to *Ppargc1a* through tail vein. Three days after the first injection, the mice were injected with indicated adenoviruses through tail vein for gain-of-function. Blood glucose levels of these mice after 16 hour fasting (n = 3 for Ad-GFP, n = 4 for Ad-P1V1 and Ad-P1V2). *J*) qPCR analyses of *Ppargc1a, P1V1*, *P1V2*, and gluconeogenic marker mRNA levels in the liver of 16 hour-fasted mice described in (*I*) (n = 3 for Ad-GFP, n = 4 for Ad-P1V1 and Ad-P1V2). *K*) PTT in 16 hour-fasted mice described in (*I*) (n = 3 for Ad-GFP, n = 4 for Ad-P1V1 and Ad-P1V2). AUC, area under the curve. *L*) qPCR analyses of *PPARGC1A* and gluconeogenic marker mRNA levels in HepG2 cells infected with indicated adenoviruses (n = 4/group). *M*) qPCR analyses of *PPARGC1A, P1V1*, *P1V2*, and gluconeogenic marker mRNA levels in HepG2 cells infected with indicated adenoviruses (n = 4/group). *N*, *O*) *Pck1* promoter activity in HepG2 cells transiently transfected with indicated vectors (n = 4/group). Data are presented as mean ± SEM. *$P < 0.05$; **$P < 0.01$; ***$P < 0.001$. n.s., not significant. 2-tailed Student's *t* test (A, D, F, L, N), 1-way ANOVA (B, E, I- K, M, O), or 2-way ANOVA (G, H).

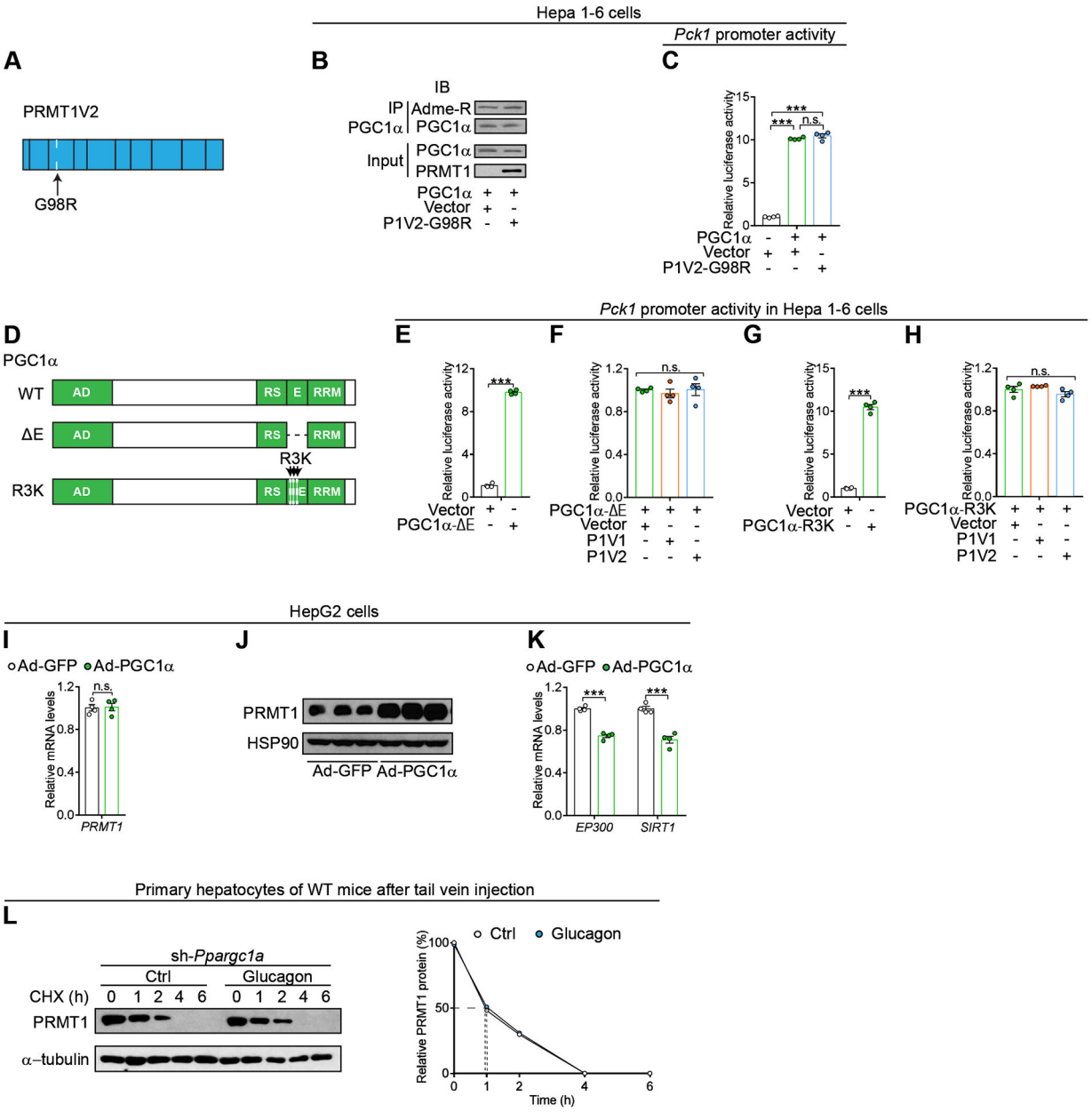

Figure 4.

PRMT1V2 activates PGC1α by asymmetric dimethylation. *A*) Schematic of PRMT1V2-G98R mutant. *B*) Analyses of asymmetric dimethylation of PGC1α. Hepa 1-6 cells were transiently transfected with indicated plasmids. Lysates were immunoprecipitated with an anti-PGC1α antibody. Both input and immunoprecipitates were analyzed by immunoblotting as indicated. *C*) *Pck1* promoter activity in Hepa 1-6 cells transiently transfected with indicated vectors (n = 4/group). *D*) Schematic of PGC1α mutants. WT, wild-type; AD, activation domain; RS, serine/arginine-rich region; RRM: RNA recognition motif. *E-H*) *Pck1* promoter activity in Hepa 1-6 cells transiently transfected with indicated vectors (n = 4/group). *I*) qPCR analyses of *PRMT1* mRNA levels in HepG2 cells infected with indicated adenoviruses (n = 4/group). *J*) Immunoblot analyses of PRMT1 in HepG2

cells described in (*I*) (n = 3/group). HSP90 was used as a loading control. *K*) qPCR analyses of *EP300* and *SIRT1* in HepG2 cells described in (*I*) (n = 4/group). *L*) Immunoblot (left) and quantification (right) analyses of PRMT1 in primary hepatocytes isolated from wild-type mice after injection with indicated adenovirus and treated with 100 μg/mL cycloheximide (CHX) for indicated time after pretreatment with vehicle (Ctrl) or 200 nM glucagon for 3 hours. α-tubulin was used as a loading control. Data are presented as mean ± SEM. ***$P < 0.001$. n.s., not significant. 2-tailed Student's *t* test (E, G, I, K) or 1-way ANOVA (C, F, H).

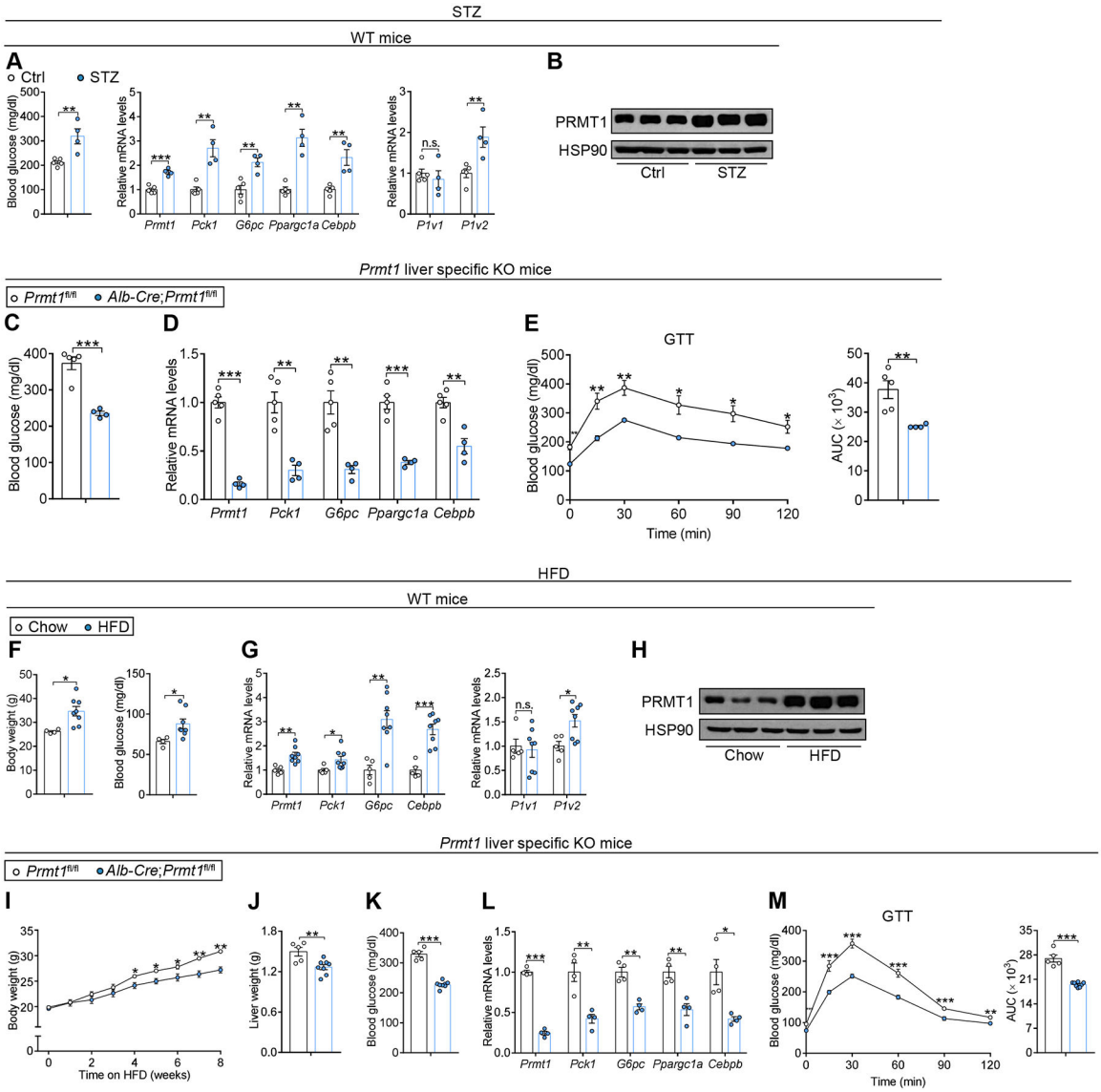

Figure 5.

Hepatocyte-specific *Prmt1* deletion ameliorates diabetic hyperglycemia. *A*) Blood glucose levels (left) and qPCR analyses of *Prmt1* and gluconeogenic marker (middle) and two different *Prmt1* variants mRNA levels (right) in the liver from wild-type (WT) mice intraperitoneally injected with vehicle (Ctrl) or 100 mg/kg streptozocin (STZ) daily for one week (n = 5 for Ctrl, n = 4 for STZ). *B*) Immunoblot analyses of PRMT1 in the liver of mice described in (*A*) (n = 3/group). HSP90 was used as a loading control. *C*) Blood glucose levels of *Prmt1*$^{fl/fl}$ and *Alb-Cre*;*Prmt1*$^{fl/fl}$ mice in the fed state after daily intraperitoneal injection with 100 mg/kg STZ for one week (n = 5 for *Prmt1*$^{fl/fl}$, n = 4 for *Alb-Cre*;*Prmt1*$^{fl/fl}$). *D*) qPCR analyses of *Prmt1* and gluconeogenic marker mRNA levels in the liver of mice in the fed state described in (*C*) (n = 5 for *Prmt1*$^{fl/fl}$, n = 4 for *Alb-Cre*;*Prmt1*$^{fl/fl}$). *E*) GTT in 16 hour-fasted mice described in (*C*) (n = 5 for *Prmt1*$^{fl/fl}$, n = 4 for *Alb-Cre*;*Prmt1*$^{fl/fl}$). AUC, area under the curve. *F*) Body weight (left) and 16 hour-fasted blood glucose levels (right) in WT mice on chow diet or high fat diet (HFD) for 12 weeks (n

= 4 for Chow, n = 8 for HFD). *G*) qPCR analyses of *Prmt1* and gluconeogenic marker (left) and two different *Prmt1* variants (right) mRNA levels in the liver from mice described in (*F*) (n = 5 for Chow, n = 8 for HFD). *H*) Immunoblot analyses of PRMT1 in the liver of mice described in (*F*) (n = 3/group). HSP90 was used as a loading control. *I*) Changes in body weights of $Prmt1^{fl/fl}$ and *Alb-Cre*;$Prmt1^{fl/fl}$ mice upon HFD (n = 5 for $Prmt1^{fl/fl}$, n = 8 for *Alb-Cre*;$Prmt1^{fl/fl}$). *J*) Liver weight of $Prmt1^{fl/fl}$ and *Alb-Cre*;$Prmt1^{fl/fl}$ mice after 8 weeks on HFD (n = 5 for $Prmt1^{fl/fl}$, n = 8 for *Alb-Cre*;$Prmt1^{fl/fl}$). *K*) Blood glucose levels in 6 hour-fasted mice described in (*J*) (n = 5 for $Prmt1^{fl/fl}$, n = 8 for *Alb-Cre*;$Prmt1^{fl/fl}$). *L*) qPCR analyses of *Prmt1* and gluconeogenic marker mRNA levels in the liver of 6 hour-fasted mice described in (*J*) (n = 4/group). *M*) GTT in 16 hour-fasted mice described in (*J*) (n = 5 for $Prmt1^{fl/fl}$, n = 8 for *Alb-Cre*;$Prmt1^{fl/fl}$). AUC, area under the curve. Data are presented as mean ± SEM. *$P < 0.05$; ** $P < 0.01$; ***$P < 0.001$. n.s., not significant. 2-tailed Student's *t* test (A, C-G, I-M).